Communication

Plasmonic Nanoparticle Chains via a Morphological, Sphere-to-String Transition

Youngjong Kang, Kris J. Erickson, and T. Andrew Taton

J. Am. Chem. Soc., **2005**, 127 (40), 13800-13801• DOI: 10.1021/ja055090s • Publication Date (Web): 17 September 2005

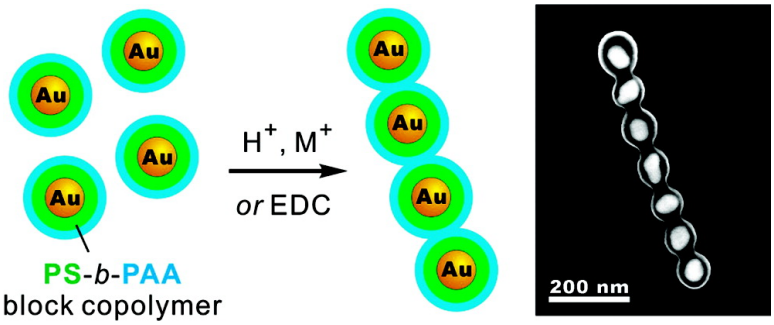

More About This Article

Additional resources and features associated with this article are available within the HTML version:

- Supporting Information
- Links to the 23 articles that cite this article, as of the time of this article download
- Access to high resolution figures
- Links to articles and content related to this article
- Copyright permission to reproduce figures and/or text from this article

View the Full Text HTML

J|A|C|S
COMMUNICATIONS

Published on Web 09/17/2005

Plasmonic Nanoparticle Chains via a Morphological, Sphere-to-String Transition

Youngjong Kang, Kris J. Erickson, and T. Andrew Taton*

Department of Chemistry, University of Minnesota, 207 Pleasant Street SE, Minneapolis, Minnesota 55455

Received July 27, 2005; E-mail: taton@chem.umn.edu

One-dimensional (1D) chains of regularly spaced, metal nanoparticles exhibit unique, coherent optical properties when the distance between particles is short enough for near-field coupling of their surface plasmon resonances.[1] For example, theoretical[2] and experimental[3] studies have shown that a 1D nanoparticle chain can serve as a "plasmon waveguide", through which optical energies can propagate even though the chain is much narrower than the diffraction limit. Surface lithography,[4,5] solution-phase templated assembly,[6] and dipolar interactions[7] have been used to fabricate plasmonically coupled nanoparticle chains, with the goal of precisely controlling particle shape and size, interparticle spacing, and chain geometry. Herein, we report that nanoparticles that have been encapsulated within cross-linked, spherical micellar shells can be induced to assemble into structurally defined chains by triggering a morphological, sphere-to-string transition in the micelle component (Scheme 1).

Previous research has shown that direct morphological transitions between spherical and wormlike block-copolymer micelles can be induced by varying solvent quality, ionic strength, or pH.[8] In addition, under special circumstances, this transition can be frustrated to yield intermediate, necklace-like structures.[9] We have found that this same frustrated transition occurs when metal nanoparticles surrounded by a layer of cross-linked, amphiphilic poly(styrene-*block*-acrylic acid) ("Au@PS-*b*-PAA")[10] are exposed to conditions that reduce interfacial curvature in the copolymer (Scheme 1). Au nanoparticles were encapsulated within PS_m-*b*-PAA_{13} (m = 100, 160, or 250), and 50% of the PAA carboxylates were cross-linked, as previously described (Table 1).[10,11] Transmission electron microscopy (TEM) images of these starting structures showed single, isolated nanoparticles surrounded by copolymer shells of uniform thickness (Figure 1a). As aqueous suspensions of these nanostructures (between 5 nM and 1 pM in particles) were gradually exposed to increasing concentrations of NaCl, $CaCl_2$, acetic acid (AcOH), or 1-(3-dimethylamino)propyl)-3-ethylcarbodiimide methiodide (EDC)—all of which induce a transition from spherical to wormlike micelles for PS-*b*-PAA alone[8]—the Au@PS-*b*-PAA nanoparticles were progressively assembled into longer and longer, 1D chains. For example, as [EDC] was titrated from 0 to ~90 μM, an aqueous suspension of Au@PS_{250}-*b*-PAA_{13} gradually turned from reddish to paler, bluish violet in color, due to aggregation of the gold nanoparticles and coupling of surface plasmon excitations.[12] TEM analysis of these aggregates (Figure 1b,c) showed that particles were assembled into chains rather than random structures, and that for [EDC] < 90 μM, more EDC led to longer chains. As EDC was added beyond [EDC] ≈ 90 μM, TEM images and visual inspection of the solution showed that the aggregates had re-dissociated into individual encapsulated Au particles. We attribute this behavior to inversion of charge at the micelle surface. In principle, micelle-bound, cationic EDC ligands initially balance the surface charge from carboxylate anions enough to allow a reduction in micelle surface curvature and the sphere-to-string morphological transition. However, too much added EDC ligand results in cationic surfaces that once again exhibit sufficient intra- and interparticle repulsion to maintain isolated, spherical particles. This process was confirmed in situ by absorption spectroscopy (Figure 1e,f), which showed a gradual red-shift in the absorption maxima characteristic of surface plasmon coupling for low to intermediate concentrations of EDC, followed by a blue-shift for higher concentrations. The sphere-to-string transition was also induced by increasing solution ionic strength to screen surface charge (NaCl), adding bridging ions ($CaCl_2$), or neutralizing dissociated carboxylates (AcOH). In all cases, the transition could be reversed by neutralizing or diluting the additive. However, when

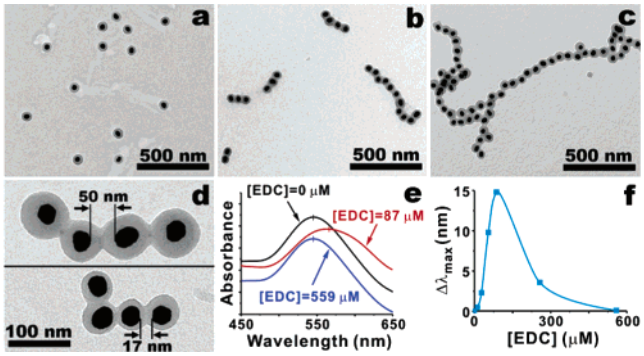

Figure 1. (a−c) TEM images of transition from spherical Au@PS_{250}-*b*-PAA_{13} (**4**, Table 1) to nanoparticle chains with increasing concentrations of EDC; [EDC] = (a) 0 μM, (b) 55 μM, (c) 87 μM. (d) TEM images of representative nanoparticle chains prepared from nanostructures with different shell thicknesses: (top) **3**; (bottom) **2**. (e) Absorption spectra of nanoparticle chains made from **4** at different concentrations of EDC. The wavelength of maximum absorption (λ_{max}) is marked on each spectrum. (f) Variation in λ_{max} with [EDC].

Scheme 1

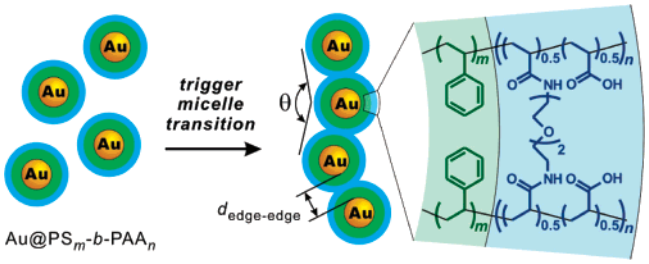

Table 1. Structural Characteristics of Nanoparticle Chains Formed from Au@PS-*b*-PAA

sample	d_{Au} (nm)	shell composition	initial t_{shell} (nm)	$d_{edge-edge}$ (nm)
1	12 ± 1	PS_{250}-*b*-PAA_{13}	14 ± 1	24 ± 2
2	32 ± 3	PS_{100}-*b*-PAA_{13}	10 ± 1	17 ± 2
3	32 ± 3	PS_{160}-*b*-PAA_{13}	28 ± 4	50 ± 6
4	32 ± 3	PS_{250}-*b*-PAA_{13}	21 ± 2	35 ± 6
5	52 ± 5	PS_{160}-*b*-PAA_{13}	16 ± 2	27 ± 3

10.1021/ja055090s CCC: $30.25

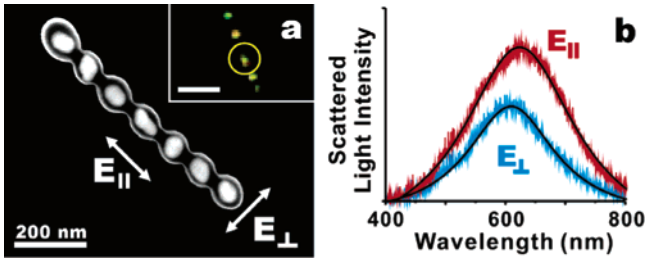

Figure 2. (a) SEM and dark-field optical microscopy (inset, scale bar represents 2 μm) images of a straight nanoparticle chain made from **5**. The sample position in the optical image is rotated 25° clockwise relative to the SEM image. (b) Scattering spectra of the chain, collected under oblique illumination with light polarized parallel ($E_{||}$) or perpendicular ($E_{\perp}$) to the long axis. Spectra were collected from the aperture-limited, circled area in the inset of (a); $\lambda_{max}(E_{||}) = 621$ nm, $\lambda_{max}(E_{\perp}) = 607$ nm. The solid lines are Lorentz fits of the spectral data.

EDC was used to induce assembly, the resulting nanoparticle strings could be locked into place by immediately adding aqueous diamine linker. This yielded permanent structures that were not affected by solution conditions.

The sphere-to-string transition yielded chains of regularly spaced nanoparticles up to ~20 μm in length. By contrast, when hydrophobic Au nanoparticles were mixed with free PS-*b*-PAA amphiphile, and solvent conditions were changed such that cylindrical micelles were assembled directly around the nanoparticles,[13] TEM images showed poorly structured combinations of micelles and particles instead.[14] This is consistent with previous efforts to directly synthesize nanoparticles within wormlike micelles, which yielded less control over interparticle spacing.[15] Some longer particle strings were branched, as is also observed for wormlike micelles.[16] Branching was sensitive to the conditions of micelle assembly and TEM sample preparation, and optimizing both of these steps improved the yield of unbranched, straight structures observed by TEM. Overall, the degree of branching in all samples was much less than that in fractal particle precipitates.[17] In addition, the average three-center angle θ (Scheme 1) for stringed particles with only two neighbors was $\geq 150°$ for all samples.[18] Most importantly, TEM images of the micelles showed that interparticle spacing was determined exclusively by the thickness of the micellar shell (t_{shell}) in the spherical starting materials. As shown in Table 1, this method was used to construct chains from different Au particle sizes, polymer shell compositions, and shell thicknesses. In all cases, the final edge-to-edge interparticle distance ($d_{edge-edge}$) was ~0.85 times the sum of the two shell thicknesses. Standard deviations in $d_{edge-edge}$ were less than 20%, and deviations in interparticle center-to-center distances were less than 10%. We argue that this consistency is due to the glassy nature of the PS copolymer block, which cannot deform during the assembly process. Because both the particle diameter and shell thickness of the Au@PS-*b*-PAA starting material can be specifically determined,[11] assembly yields 1D nanoparticle arrays with precise structural control.

Far-field, polarized microspectroscopy has been previously used to analyze unidirectional near-field plasmon coupling in nanostructure arrays,[5,20] and we chose to use this method to test the potential of micelle-templated assemblies for use as 1D optical conduits. Nanoparticle chains were straightened by depositing a droplet of warm suspension onto a silicon wafer and allowing it to dry. Structural combing[21] at the drying droplet edge led to straightening of the particle chains, as verified by SEM imaging. One particular chain which could be reproducibly located in terms of surface markers was chosen for analysis by SEM (Figure 2a), dark-field optical microscopy (Figure 2a, inset), and polarized scattering (dark-field) microspectroscopy (Figure 2b). Scattering spectra of this single chain with different polarizations of incident light showed significantly different intensities and wavelength maxima, indicating directional surface plasmon coupling.[5]

In conclusion, we have demonstrated a facile method of spontaneously assembling plasmonic Au nanoparticle chains which takes advantage of a morphological micelle transition. We are currently investigating the effects of particle size, composition, and spacing on directional plasmon coupling in more detail, with the goal of constructing plasmon waveguides with tunable interparticle coupling by solution-phase self-assembly. We propose that this method provides a simple avenue to investigate the unique optical properties of 1D nanoparticle arrays for future optoelectronic device applications.[22]

Acknowledgment. This work was supported by the Alfred P. Sloan Foundation (Fellowship BR-4527 to T.A.T.) and the ACS Petroleum Research Fund (38303-G5).

Supporting Information Available: Detailed synthetic procedures and experimental details for far-field polarization spectroscopy, TEM, and SEM images for other Au nanoparticle chains. This material is available free of charge via the Internet at http://pubs.acs.org.

References

(1) (a) Zhao, L.; Kelly, K. L.; Schatz, G. C. *J. Phys. Chem. B* **2003**, *107*, 7343−7350. (b) Quinten, M. *J. Cluster Sci.* **1999**, *10*, 319−358. (c) Kreibig, U.; Vollmer, M. *Optical Properties of Metal Clusters*; Springer: Berlin, 1995.
(2) (a) Citrin, D. S. *Nano Lett.* **2004**, *4*, 1561−1565. (b) Weber, W. H.; Ford, G. W. *Phys. Rev. B: Condens. Matter Mater. Phys.* **2004**, *70*, 125429. (c) Brongersma, M. L.; Hartman, J. W.; Atwater, H. A. *Phys. Rev. B: Condens. Matter Mater. Phys.* **2000**, *62*, R16356−R16359. (d) Quinten, M.; Leitner, A.; Krenn, J. R.; Aussenegg, F. R. *Opt. Lett.* **1998**, *23*, 1331−1333.
(3) Maier, S. A.; Kik, P. G.; Atwater, H. A.; Meltzer, S.; Harel, E.; Koel, B. E.; Requicha, A. A. G. *Nat. Mater.* **2003**, *2*, 229−232.
(4) (a) Salerno, M.; Krenn, J. R.; Hohenau, A.; Ditlbacher, H.; Schider, G.; Leitner, A.; Aussenegg, F. R. *Opt. Commun.* **2005**, *248*, 543−549. (b) Quidant, R.; Leveque, G.; Weeber, J. C.; Dereux, A.; Girard, C.; Weiner, J. *Europhys. Lett.* **2004**, *66*, 785−791.
(5) (a) Wei, Q. H.; Su, K. H.; Durant, S.; Zhang, X. *Nano Lett.* **2004**, *4*, 1067−1071. (b) Gunnarsson, L.; Rindzevicius, T.; Prikulis, J.; Kasemo, B.; Kaell, M.; Zou, S.; Schatz, G. C. *J. Phys. Chem. B* **2005**, *109*, 1079−1087.
(6) (a) Deng, Z.; Tian, Y.; Lee, S.-H.; Ribbe, A. E.; Mao, C. *Angew. Chem., Int. Ed.* **2005**, *44*, 3582−3585. (b) Le, J. D.; Pinto, Y.; Seeman, N. C.; Musier-Forsyth, K.; Taton, T. A.; Kiehl, R. A. *Nano Lett.* **2004**, *4*, 2343−2347. (c) Warner, M. G.; Hutchison, J. E. *Nat. Mater.* **2003**, *2*, 272−277.
(7) Tang, Z.; Ozturk, B.; Wang, Y.; Kotov, N. A. *J. Phys. Chem. B* **2004**, *108*, 6927−6931.
(8) Zhang, L.; Eisenberg, A. *Macromolecules* **1996**, *29*, 8805−8815.
(9) Ma, Q.; Remsen, E. E.; Clark, C. G., Jr.; Kowalewski, T.; Wooley, K. L. *Proc. Natl. Acad. Sci. U.S.A.* **2002**, *99*, 5058−5063.
(10) Kang, Y.; Taton, T. A. *Angew. Chem., Int. Ed.* **2005**, *44*, 409−412.
(11) Kang, Y.; Taton, T. A. *Macromolecules* **2005**, *38*, 6115−6121.
(12) (a) Kelly, K. L.; Coronado, E.; Zhao, L. L.; Schatz, G. C. *J. Phys. Chem. B* **2003**, *107*, 668−677. (b) Su, K. H.; Wei, Q. H.; Zhang, X.; Mock, J. J.; Smith, D. R.; Schultz, S. *Nano Lett.* **2003**, *3*, 1087−1090.
(13) Yu, Y. S.; Eisenberg, A. *J. Am. Chem. Soc.* **1997**, *119*, 8383−8384.
(14) See Supporting Information for further details of synthesis and characterization.
(15) (a) Duxin, N.; Liu, F.; Vali, H.; Eisenberg, A. *J. Am. Chem. Soc.* **2005**, *127*, 10063−10069. (b) Wang, X.-S.; Wang, H.; Coombs, N.; Winnik, M. A.; Manners, I. *J. Am. Chem. Soc.* **2005**, *127*, 8924−8925.
(16) Jain, S.; Bates, F. S. *Science* **2003**, *300*, 460−464.
(17) Weitz, D. A.; Oliveria, M. *Phys. Rev. Lett.* **1984**, *52*, 1433−1436.
(18) TEM-imaged structures do not necessarily represent structures in suspension. We propose that solution structures are likely less perturbed—i.e., straighter, and possibly less branched—than those deformed by physical deposition onto TEM grids.
(19) Link, S.; El-Sayed, M. A. *J. Phys. Chem. B* **2005**, *109*, 10531−10532.
(20) Maier, S. A.; Kik, P. G.; Atwater, H. A. *Appl. Phys. Lett.* **2002**, *81*, 1714−1716.
(21) Bensimon, A.; Simon, A.; Chiffaudel, A.; Croquette, V.; Heslot, F.; Bensimon, D. *Science* **1994**, *265*, 2096−2098.
(22) Atwater, H. A.; Maier, S.; Polman, A.; Dionne, J. A.; Sweatlock, L. *MRS Bull.* **2005**, *30*, 385−389.

JA055090S